Computer-Aided Design 79 (2016) 12–26

Contents lists available at ScienceDirect

Computer-Aided Design

journal homepage: www.elsevier.com/locate/cad

Hierarchical grid conversion

Ali Mahdavi-Amiri *, Erika Harrison, Faramarz Samavati

Department of Computer Science, University of Calgary, 2500 University Drive N.W., Calgary, Alberta, Canada T2R1S4

ARTICLE INFO

Article history:
Received 21 January 2015
Accepted 9 April 2016

Keywords:
Refinements
Grid conversion
Patch-based data structures
Transformations
Semiregular
Subdivision

ABSTRACT

Hierarchical grids appear in various applications in computer graphics such as subdivision and multiresolution surfaces, and terrain models. Since the different grid types perform better at different tasks, it is desired to switch between regular grids to take advantages of these grids. Based on a 2D domain obtained from the connectivity information of a mesh, we can define simple conversions to switch between regular grids. In this paper, we introduce a general framework that can be used to convert a given grid to another and we discuss the properties of these refinements such as their transformations. This framework is hierarchical meaning that it provides conversions between meshes at different level of refinement. To describe the use of this framework, we define new regular and near-regular refinements with good properties such as small factors. We also describe how grid conversion enables us to use patch-based data structures for hexagonal cells and near-regular refinements. To do so, meshes are converted to a set of quadrilateral patches that can be stored in simple structures. Near-regular refinements are also supported by defining two sets of neighborhood vectors that connect a vertex to its neighbors and are useful to address connectivity queries.

1. Introduction

Triangular, quadrilateral, and hexagonal grids appear in many applications in computer graphics such as finite elements, subdivision and multiresolution surfaces, and terrain rendering. Triangular grids are common due to their application in many fundamental algorithms such as Delaunay triangulation and Loop subdivision [1,2], and they are also optimized for processing on modern hardware. The simple parametric form of quadrilateral grids can be readily applied to tensor product surfaces, NURBS, B-Spline, and Catmull–Clark patches [3,4]. Furthermore, quadtrees [5] exploit the simple boundaries of quadrilateral grids and their straightforward hierarchical shape. Hexagonal grids provide the best sampling of surfaces as they provide less bias towards edges (they are more circular) in comparison with squares and triangles, support uniform neighborhood, and provide a reduced quantization error over other alternatives [6]. As a result, hexagonal grids appear in applications such as hierarchical representation of the Earth and subdivision surfaces [7,8].

In this paper, we provide hierarchical grid conversions between triangular, quadrilateral and hexagonal grids. These conversions are basically simple modifications in the connectivity of vertices that convert a type of grid to another. Using these conversions, we can switch between the grids as the need dictates (see Fig. 1). For example, hierarchical shapes resulting from a refinement of quads are very simple as opposed to hexagons that are not congruent (this means that it is not possible to completely cover a hexagon by a set of complete and disjoint smaller hexagons). As a result, we can convert hexagonal grids to quadrilaterals to design an efficient data structure for hexagonal grids and benefit from the simple hierarchical shape of quads and convert them back when cells with better sampling rate or a uniform neighborhood definition are desired.

Hierarchy among the cells is typically provided by refinements. Refinements introduce more cells and vertices into a model. When a refinement is applied to a cell with area A, it divides the cell into some smaller cells with area $\frac{A}{i}$. Such a refinement is called 1-to-i refinement or a refinement with the factor of i [9]. Refinements are useful when i is an integer number since after two levels of subdivision the cells are simply scaled by an integer number (although lattices may not be aligned). However, these refinements are typically specified for a particular grid. For instance, quadrilateral 1-to-3 refinement has not been defined while triangular 1-to-3 refinement has been successfully employed in $\sqrt{3}$ subdivision. Using hierarchical grid conversions, we propose a framework to define such refinements and study their properties.

* Corresponding author.
E-mail addresses: amahdavi@ucalgary.ca (A. Mahdavi-Amiri), eharris@ucalgary.ca (E. Harrison), samavati@ucalgary.ca (F. Samavati).

http://dx.doi.org/10.1016/j.cad.2016.04.005
0010-4485/

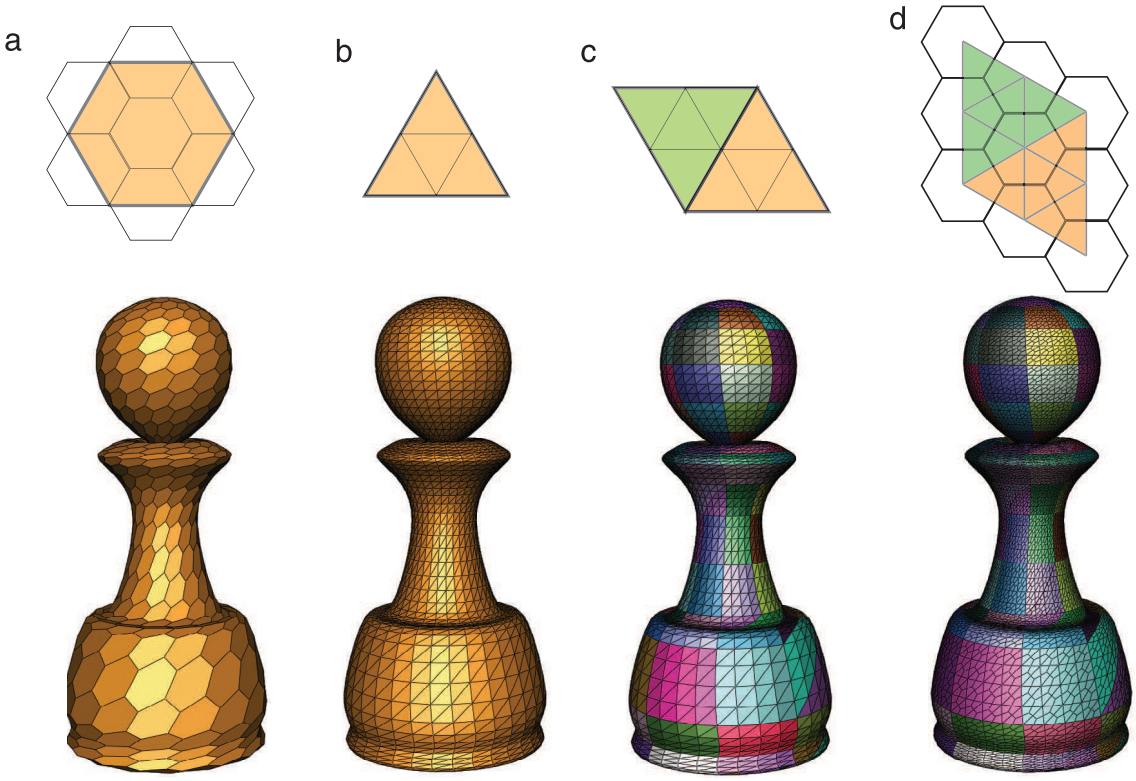

Fig. 1. Semiregular hexagonal and triangular models ((a) and (b) at the bottom) are created by hexagonal and triangular refinements ((a) and (b) at the top). Using conversions such as pairing ((c) at the top), or dual ((d) at the top), we can use simple quadrilateral hierarchical shapes and efficient data structures for packing models in (a) and (b) at the bottom into quadrilateral patches ((c) and (d) at the bottom).

Contributions

Our main contribution is to present hierarchical conversions between regular grids. To demonstrate the usefulness of these conversions, we use them to define new near-regular and regular refinements for grids and extend an existing patch-based hierarchical data structure – Atlas of Connectivity Maps (ACM) – [10,11] to support hexagonal grids and more variety of regular and near-regular refinements.

2. Related work

As we present hierarchical grid conversions in this paper and use them to define new refinements and hierarchical data structures, we can categorize the work related to our method into three groups: conversions between regular grids, refinement and subdivision, and data structures proposed to support multiresolution (hierarchy) of semiregular models. In the following, we provide prior work of each group.

2.1. Conversion between regular grids

Grid conversion is already well explored within the Computer Graphics community, under the topic of remeshing. Triangulation [12,13] and quadrangulation [14] convert arbitrary meshes to those with cells, of triangles and quadrilaterals respectively. This remeshing may improve rendering time, mesh quality, or fulfill geometric or aesthetic constraints. Hexagonal remeshing occurs for architectural reasons or to better represent features on the mesh due to the better sampling property [15–18]. Alternatively, conversions can occur through duality remeshing to achieve a specific cell type [8], or improve smoothness [19].

These cell conversions mostly take complicated geometric properties (e.g. Gaussian curvature) into consideration for converting one type of grid to another as their applications need to satisfy a specific geometric property [14]. However, we convert the grids on 2D domains by simple operations that only change the connectivity of vertices. Some of these conversions are very straightforward. However, we combine them with refinements to define new refinements and design efficient hierarchical data structures.

2.2. Refinements

Regular refinements in surface modeling are the process of splitting faces into a set of smaller faces. After refinements, more faces and vertices are created and a higher resolution model is obtained. As a result, refinements can create a hierarchy of objects at different resolutions (i.e. the level of refinement). Regular refinements have many usages in computer graphics such as subdivision in which faces are initially split by a regular refinement and then vertices are geometrically modified to obtain a smooth surface.

Regular refinements are defined differently in literature. Guskov et al. [20] consider only the dyadic refinement as a regular quadrilateral refinement in which a face is split into four faces (Fig. 2(b)). Weiss and De Floriani [9] also consider the same definition for triangular faces. This type of refinement is the most common refinement as it is employed in designing popular subdivision methods such as Catmull–Clark and Loop [4,2] and useful data structures such as quadtrees [5].

Velho in [21] defines regular refinements for quadrilateral meshes as a process that produces a finer set of similar faces that are only scaled. He then categorizes regular refinements as *primal* and *dual*. In a primal subdivision, the vertices of the coarse tessellation are preserved and old edges are divided and reconnected while in a dual subdivision, new vertices are inserted in the interior of

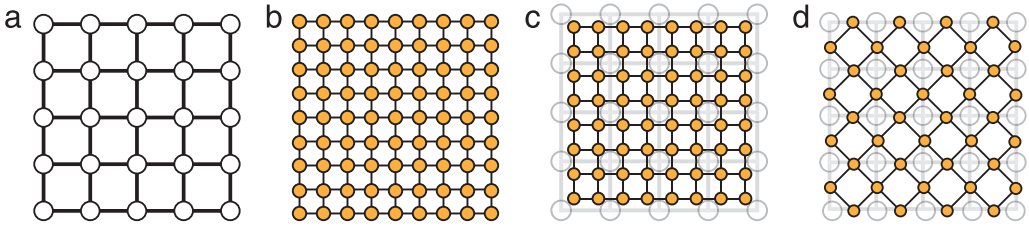

Fig. 2. (a) A set of coarse points. (b) Dyadic refinement. (c) Doo–Sabin refinement. (d) Simplest refinement.

faces and the old vertices and edges are discarded. With this definition Doo–Sabin refinement is a regular dual refinement (Fig. 2(c)). However, there still exist some regular refinements that are not included in this definition. Simplest refinement [22] in which new vertices are inserted at edges and the old vertices and edges are discarded is an example of a regular refinement that does not cover by Velho's definition (Fig. 2(d)).

Alexa [23] defines the regular refinements using 2D regular triangular meshes. He considers a coordinate system for triangle meshes using two edges of an equilateral triangle. To study the behavior of refinements, he establishes the hierarchical relationship between the coordinate system of triangular meshes before and after refinements.

As noted by Ivrissimtzis et al. [24], the definition of Alexa for 2D triangular meshes can be rephrased as 2D triangular lattices. If a 2D regular triangular lattice is named L_0, after an application of a regular refinement, a higher resolution lattice L_1 is created, and after r applications of a regular refinement L_r is made. Regular refinements studied by Alexa have three conditions as the following:

- All the lattices are similar (all triangles are equilateral).
- Lattice L_{n+1} can be obtained using a transformation in the Euclidean plane and the scale of the transformation is called *arity* of the refinement.
- Point sets of a lattice with higher resolution is the superset of the point set of a lower resolution (i.e. $L_0 \subset L_1 \subset L_2 \cdots \subset L_n$).

Ivrissimtzis et al. [24] use the same concept for categorizing refinements for regular quadrilateral lattices. However, the third condition in the Alexa's definition excludes dual refinements such as Doo–Sabin since in such a refinement the old vertices are discarded ($L_r \not\subset L_{r+1}$). As a result, they replace the third condition with a looser one in which they consider both center-faces, and the vertices of L_{r+1}, as valid locations for the points of the coarser lattice L_r.

The usefulness of these refinements is later examined through a set of heuristics by Dodgson in [25]. Destelle et al. [26] also defined a set of subdivision operators. Using these operators, some regular and irregular refinements can be produced. However, there exists an intermediate set of refinements that are not completely irregular but they are not also regular. An example of such a refinement is the 1-to-2 refinement employed in 4–8 subdivision which carries good properties such as C^4 continuity at regular vertices. In this paper, we introduce new regular and near-regular refinements by proposing a simple framework and study some of their properties. We hope that these refinements can later provide useful smooth subdivision schemes although subdivision schemes are not the only application of refinements. An alternative example of the refinements' application is Earth representation in which a hierarchical model is created by combining refinement and spherical projection [27,7,28].

2.3. Multiresolution data structures

Multiresolution surfaces have applications in mesh editing, compression, and morphing. One approach to construct multiresolution is to use surface subdivision (or refinement) [29,30]. Various data structures support subdivision and multiresolution surfaces [9], with the most common keeping the connectivity information of vertices and faces into each edge [31,32]. Unfortunately, these data structures require an excessive amount of memory and time to represent and maintain high resolution objects and their hierarchy.

To support subdivision and multiresolution surfaces, hierarchical data structures such as quadtrees are more useful [5]. In order to make quadtrees more efficient, indexing methods in which a unique index is assigned to each node have been proposed. Connectivity queries are then handled using a defined algebra on the indices themselves [5,33,34]. Hierarchical indexing methods can be efficient in terms of both space and time.

In some multiresolution frameworks, meshes have to be semiregular or they must have subdivision connectivity [14,30,35]. These models are obtained by applying repetitive refinement on a mesh with an arbitrary topology. The result of this operation is a model composed of a set of connected regular cells. A patch usually refers to an $m \times n$ block of quads (possibly $m \neq n$) connected to each other. By this definition, all the internal vertices are regular, all vertices along the boundary edges have valence three except four vertices at the corners that have valence two. Patches can be defined similarly for triangular and hexagonal patches. The only difference is the valence of internal boundary and corner vertices. For example, an internal vertex in a triangular patch has valence six while corner vertices have valence two or three and boundary vertices have valence four. Recently, Mahdavi-Amiri and Samavati proposed an Atlas of Connectivity Maps (ACM) an indexing method to support semiregular quadrilateral and triangular multiresolution objects [36,11]. Using conversions between regular grids, we can adapt ACM to additionally support hexagonal models. Conversions between grids not only enable us to adapt ACM but we can also adapt other indexing methods defined for quadtrees or similar structures featuring different properties to support all regular grids.

3. Conversion between regular grid systems

By changing the connectivity of cells or applying simple operations, we can convert one type of a regular grid to another. These conversions can be then used to define novel refinements or extend hierarchical data structures to support cells with complicated hierarchy definitions such as hexagons.

An important property of a regular grid is that the connectivity of cells and vertices are implicit and there is no need to explicitly store the connection of cells or vertices. Each cell has a corresponding face with 3D vertices that can be obtained by mapping ϕ. ϕ can be defined via numerous sources such as B spline surfaces, subdivision masks, or explicitly storing the location of

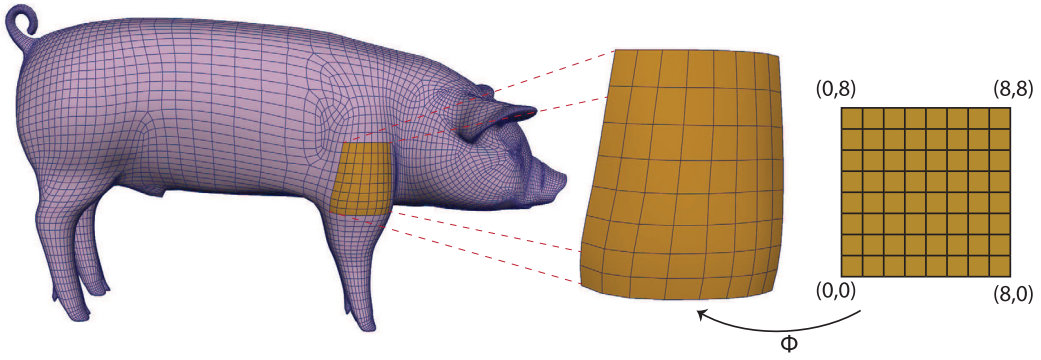

Fig. 3. An eight by eight 3D patch on a mesh that is mapped to a 2D grid.

vertices. A patch is a 2D regular grid mapped onto a 3D surface (see Fig. 3). Similar to the coordinate systems of lattices [24], we define the coordinate systems on the regular grids (2D domains) by taking one vertex as the origin and two incident edges to be the coordinate axes [24,23]. This coordinate system provides an integer indexing that can be used within a data structure to address a 2D array storing the 3D locations of each vertex (acting as ϕ).

Grid G_i, $i \in \{t, q, h\}$ denotes triangular, quadrilateral, or hexagonal when i is t, q, or h respectively. Given a grid G_i, we can convert it to grid G_j $j \in \{t, q, h\}$ by conversion $C^{i\to j}$. $C^{i\to j}$ is an operation applied on the connectivity of a given mesh by inserting new vertices or edges or removing the existing ones. These conversions are defined on the 2D domain of the mesh that are obtained by mapping vertices to a set of 2D coordinates with integer indices. In these 2D domains, G_i and G_j have their own coordinate systems (O_i, U_i, V_i) and (O_j, U_j, V_j). In these coordinate systems, O is the origin chosen as one of the vertices on the 2D domain and U and V are two edges chosen as the main axes of the coordinate system. Having such coordinate systems, it is possible to find a transformation $T^{i\to j}$ mapping (O_i, U_i, V_i) to (O_j, U_j, V_j) (Fig. 4). $T^{i\to j}$ is found through an algebraic relationship between axes of (O_i, U_i, V_i) and (O_j, U_j, V_j). Using $T^{i\to j}$, the coordinate of any point in the coordinate system of G_i can be found in G_j. In this paper, we derive some important transformation as examples. Although choosing coordinate systems on 2D domains can be arbitrary, the method for finding the transformation is the same while the resulting transformations may be slightly different. In the following sections, we introduce some conversions as well as the notations used throughout the paper. These simple conversions enable one to switch between regular grids to benefit from the advantages offered by different grids.

3.1. Pairing conversion

This conversion is basically a simple *pairing triangles* and denoted by $C_P^{t\to q}$ as the subscript refers to the name of conversion (pairing) and the superscript denotes that it converts triangular grids to quadrilaterals. Here, we first define the notation and then provide the conversion.

A quadrilateral grid G_q consists of a set C_q of quad cells with four vertices (Fig. 5). A vertex O of G_q is chosen as the origin and edges U_q and V_q incident with O_q form axes of G_q. To distinguish between indexing cells and vertices, we use $q(a, b)$ as the index of a vertex and $q[a, b]$ as the index of a cell. A vertex v in G_q has index $q(a, b)$ where (a, b) is the integer coordinate of v in (O_q, U_q, V_q). A quad cell has index $q[a, b]$ if its vertices have indices $q(a, b)$, $q(a + 1, b)$, $q(a, b + 1)$, and $q(a + 1, b + 1)$.

Similarly, to define a coordinate system for a triangular grid G_t, (O_t, U_t, V_t) illustrated in Fig. 5(d) is used. There exist two triangular cells associated with vertex $t(a, b)$. Hence, we add a superscript

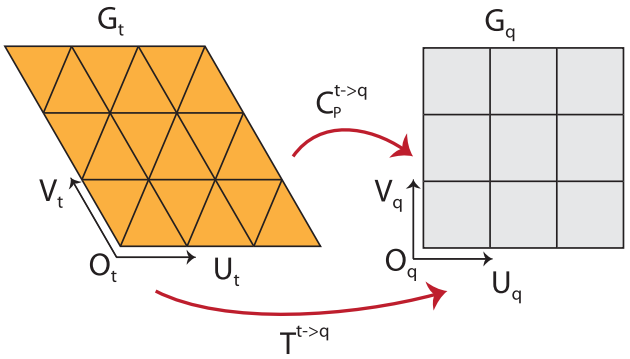

Fig. 4. Grid G_t is converted to G_q by conversion $C_P^{t\to q}$ and (O_t, U_t, V_t) is mapped to (O_q, U_q, V_q) by $T^{t\to q}$.

to differentiate between them: $t[a, b]^0$ and $t[a, b]^1$ illustrated in Fig. 5. Using this notation, two triangular cells $t[a, b]^0$ and $t[a, b]^1$ can be paired to a quad $q[a, b]$ if the edge connecting $t(a, b)$, and $t(a + 1, b + 1)$ is removed (Fig. 5(d)). This conversion from triangular cells to quads is called the *pairing conversion*.

When a mesh is closed, a complete pairing of triangles is possible and is computable in $O(M \log^4 M)$ where M is the number of triangles [37,38]. However, if the mesh has boundary, we may have some isolated triangles. Based on the application, different treatments can be applied on such triangles, we can add a dummy vertex to quadrangulate isolated triangles, if the mesh has to be pure quad (e.g. quadrilateral refinements) or we can keep them as isolated triangles but distinguish them by a flag when pairing is only needed to pack triangles for efficiency (e.g. designing an efficient data structure).

3.2. Unpairing conversion

Unpairing conversion $C_U^{q\to t}$ is the inverse of $C_P^{t\to q}$. Given quadrilateral grid G_q, connect all vertices $q(a, b)$ to $q(a + 1, b + 1)$ and obtain a triangular grid G_t. We can also define this conversion by connecting vertices along $q(a + 1, b)$ to $q(a, b + 1)$. We refer to the first case by referring to $C_U^{q\to t}$ unless otherwise is indicated. The unpairing conversion can be applied on any quadrilateral mesh as each quad can be split into two triangles. The unpairing conversion must be compatible with the pairing conversion if we want to have unpairing conversion as the inverse of the pairing conversion. This means that if vertices at the diagonal in triangle pairs have indices $q(a, b)$ to $q(a + 1, b + 1)$ in pairing conversion, in the unpairing conversion, the same vertices must be connected to each other.

3.3. Dual conversion

Hexagonal grids have also applications in parametrization, Earth representation, and surface modeling. A simple way to obtain

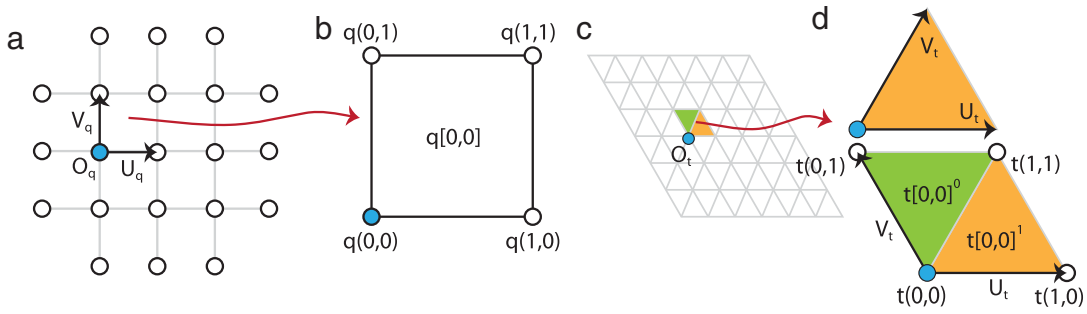

Fig. 5. (a) A quadrilateral grid, its origin O, and two axes U_q and V_q. (b) Indices of vertices of a quadrilateral cell $q[0, 0]$. (c) A triangular grid and its origin O. (d) Top: two axes U_t and V_t with 60° difference. Bottom: U_t and V_t with 120° difference, and indices corresponding to these axes for cells and vertices. Green and orange cells have indices $t[0, 0]^0$ and $t[0, 0]^1$ respectively. (For interpretation of the references to color in this figure legend, the reader is referred to the web version of this article.)

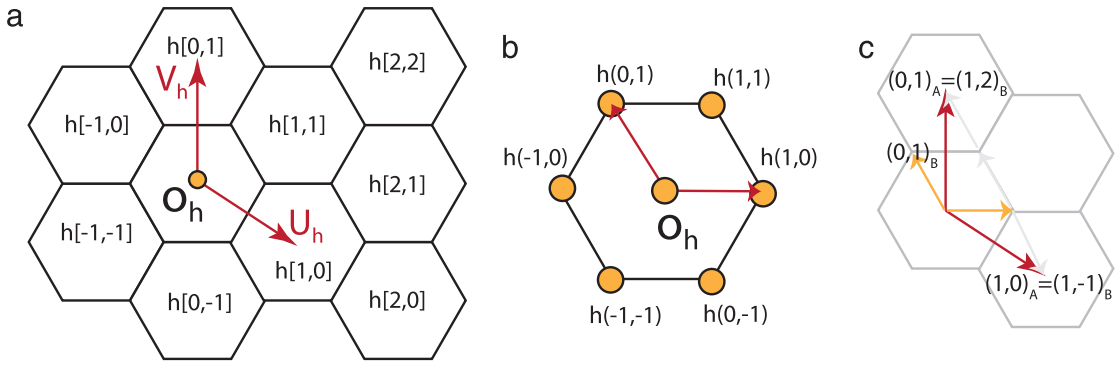

Fig. 6. (a) Hexagonal coordinate system and its corresponding indices for hexagonal cells. (b) Coordinate system to index vertices and its corresponding indices. (c) Equality of vectors in coordinate systems of (a) and (b).

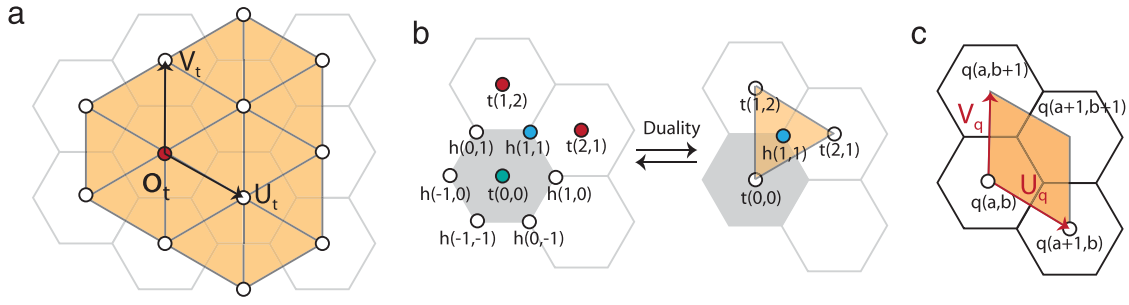

Fig. 7. (a) Dual conversion of hexagons to triangles. (b) Duality conversion between triangles and hexagons. (c) A quad corresponding to hexagonal grids, its axes and indices of its vertices.

hexagonal grids is taking the dual of triangular grids $C_D^{t\to h}$. To index hexagonal cells, we use the *hexagonal coordinate system* [39,40] (Fig. 6(a)). The origin O_h is chosen as the midpoint of an arbitrary hexagonal cell h and axes U_h and V_h have 120° difference connecting O_h to the midpoints of two neighboring cells.

A hexagonal cell gets index $h[a, b]$, if its midpoint is a and b steps from O_h along U_h and V_v respectively. Using (O_h, U_h, V_h) to index vertices does not provide our desired integer indices. Therefore, a second coordinate system for hexagonal vertices is defined (see Fig. 6(b)). Note that coordinate systems provided in Fig. 6(a) and (b) can be simply converted to each other. We use subscripts A and B to distinguish coordinates of two systems illustrated in Fig. 6(a) and (b) respectively. As illustrated in Fig. 6(c), $(1, -1)_B = (1, 0)_A$ and $(1, 2)_B = (0, 1)_A$. As a result, mapping M that transforms arbitrary coordinates $(\omega, \lambda)_B$ to $(\Omega, \Lambda)_A$ can be found by solving the system $M\begin{pmatrix}1 & 1\\ -1 & 2\end{pmatrix} = \begin{pmatrix}1 & 0\\ 0 & 1\end{pmatrix}$. Solving this system results $M = \begin{pmatrix}\frac{2}{3} & -\frac{1}{3}\\ \frac{1}{3} & \frac{1}{3}\end{pmatrix}$.

To convert hexagonal grid G_h to a triangular grid G_t ($C_D^{h\to t}$), we triangulate the hexagonal cells by forming edges between the midpoints of all adjacent hexagons (Fig. 7(a)). Similarly, to define $C_D^{t\to h}$, the midpoints of triangular cells — are taken to be the vertices of the hexagonal cells, and edges are constructed by connecting the midpoints of adjacent triangles. Note that the combination of two iterations of the dual conversion is identity. Assume that we have chosen coordinate system of Fig. 6(b) to index the vertices. We take the average of coordinates to find the midpoints. Fig. 7(b) shows that averaging points on the hexagon with vertices $h(1, 1)$, $h(1, 0)$, $h(0, 1)$, $h(-1, 0)$, $h(-1, -1)$, and $h(0, -1)$ results in vertices on triangles $(t(0, 0))$ and averaging vertices of triangles returns back the vertices of hexagons (e.g. $(\frac{t(1,2)+t(0,0)+t(2,1)}{3} = h(1, 1))$). After finding G_t from G_h by the dual conversion, one can pair the triangles and obtain a quadrilateral grid (Fig. 7(c)).

In the dual conversion, the coordinates of cells in G_h correspond to the coordinate of vertices in G_t (Fig. 8). In other words, for any vertex $t(a, b)$ in G_t, there exists a hexagonal cell with index $h[a, b]$ in G_h. As each triangular cell in G_t corresponds to a vertex in G_h, vertices of hexagonal cells can be indexed using the indices of six triangular cells (Fig. 8(d)). As a result, we employ the coordinate system in Fig. 6(a) to index hexagonal cells and

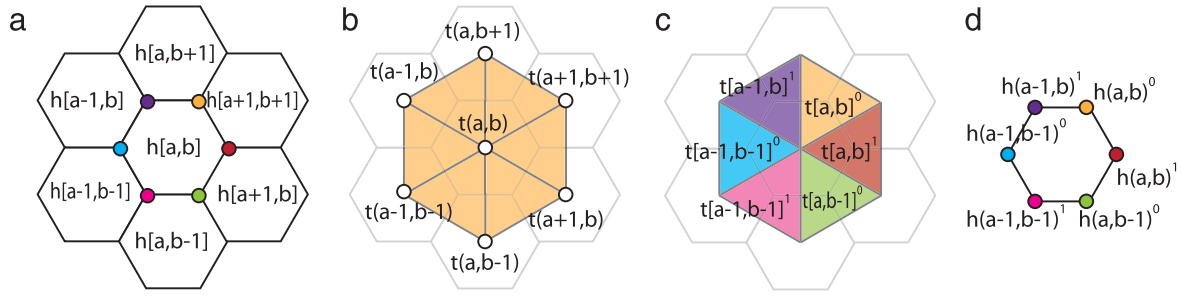

Fig. 8. (a) Indices of hexagonal cells shown by $h[]$. (b) Triangular grid of (a) obtained by dual conversion and the indices of its vertices shown by $t()$. (c) Indices of the same triangular cells in (b) shown by $t[]$. (d) Indices of vertices of the hexagonal cell $h[a, b]$ shown by $h()$.

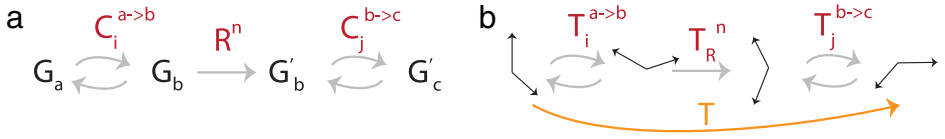

Fig. 9. (a) General framework of having conversions and refinements. (b) Having a defined coordinate system for a grid, transformations are imposed by grid conversions and refinements. R is the refinement and T is the composition of all transformations.

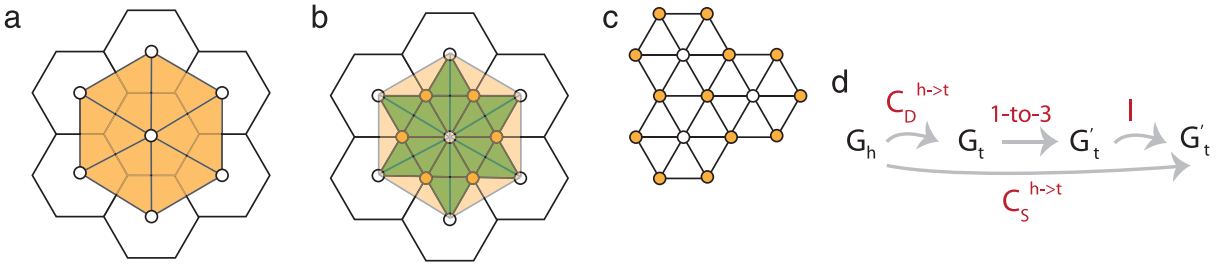

Fig. 10. (a) Hexagonal grid G_h and triangular grid G_t obtained from dual conversion $C_D^{h\to t}$. (b) 1-to-3 refinement applied on G_t to obtain $\acute{G}_t$. (c) Split conversion $C_S^{h\to t}$. (d) $C_S^{h\to t}$ is made using the multiresolution framework.

triangular vertices that are the dual of each other. Using the index of triangular vertices, we can index triangular cells similar to the case of unpairing conversion in Fig. 5(d). Finally, using the index of triangular cells, we have indexed hexagonal cells using the duality (Fig. 8).

We can apply dual conversion on any mesh. For example, the dual conversion of a regular quadrilateral mesh ($C_D^{q\to q}$) is a translated regular quadrilateral mesh. We should just note that irregular vertices on a triangular mesh would be non-hexagonal faces in the dual mesh with sides equal to the valence of vertices. Non-hexagonal faces also become extraordinary vertices when the dual conversion is applied on a hexagonal mesh. Note that faces at the boundary of a hexagonal mesh become boundary vertices in the triangular mesh after applying dual conversion on a triangular mesh.

4. Hierarchical grid conversion

Various refinements can be applied to an object in order to obtain a more detailed or smoother object. To benefit from each grid at different levels of refinement, we combine conversions and refinements within the hierarchical grid conversion (Fig. 9). Conversions and refinements may impose a transformation on the grid coordinates. Therefore, a total transformation T exists for the hierarchical grid conversion that is the composition of all involved transformations ($T = T_i^{a\to b} \circ T_R^n \circ T_j^{b\to c}$).

Using this framework, we can define useful operations and concepts. For instance, we can obtain new conversions, refinements, hierarchies, and data structures for grids. In the following, we discuss usability and applications of this framework and provide some examples.

4.1. Split and aggregation conversion

Our hierarchical grid conversions can be a base to define new conversions. In this section, we derive another conversion called *split conversion* ($C_S^{h\to t}$) (Fig. 10). To define this conversion, first G_h is converted to G_t by dual conversion $C_D^{h\to t}$ and then a 1-to-3 refinement is applied to G_t to get a higher resolution grid ($\acute{G}_t$), (see Appendix B). Note that the last conversion is identity (I) to show that it is compatible with the multiresolution framework (see Fig. 10(d)). The whole process converting G_h to $\acute{G}_t$ is split conversion. In fact, the set of all midpoints and vertices of G_h is triangulated by connecting the midpoint of each hexagonal cell to its vertices (Fig. 11). It is possible to derive the transformation T imposed by the hierarchical grid conversion. Here, we derive the transformation imposed by $C_S^{h\to t}$. $\acute{G}_t$ has the same origin as G_h and can take U_t and V_t as the basis vectors. We can find transformation mapping these grid coordinate systems by finding the equality of axes of each coordinate system. In this case, $U_h = U_t - V_t$ and $V_h = U_t + 2V_t$ (Fig. 11(c)). Then, a hexagonal cell with index $h[a, b]$ has a midpoint on vertex $t(c, d)$ in $\acute{G}_t$ where $(c, d) = \left(\begin{smallmatrix}1 & 2\\ -1 & \end{smallmatrix}\right)\left(\begin{smallmatrix}a\\ b\end{smallmatrix}\right) = (a + b, 2b - a)$. Other transformations could be defined similarly.

We can also define *aggregation conversion* denoted by $C_A^{t\to h}$ that reduces the resolution by replacing triangular cells sharing a common vertex into one cell. Vertices of h are found by adding six vectors as shown in Fig. 12(b). Note that choosing different origins in $\acute{G}_t$ results in different G_h available in three distinct configurations as illustrated in Fig. 12(c). One of these variations of aggregation conversion is the inverse of the split conversion. In Fig. 12(c), if we choose the red vertex as the origin of the aggregation conversion,

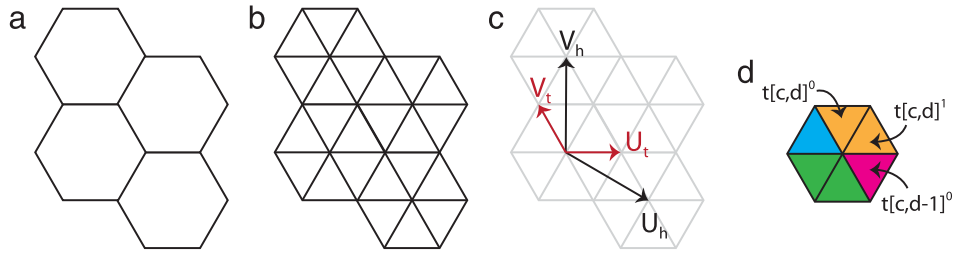

Fig. 11. (a) Part of a hexagonal grid G_h. (b) Triangulation of (a) by split conversion to get $\acute{G}_t$. (c) Coordinate systems of G_h, and $\acute{G}_t$ illustrated by black and red arrows respectively. (d) A hexagonal cell is converted into six triangular cells. Indices of some triangular cells are shown. (For interpretation of the references to color in this figure legend, the reader is referred to the web version of this article.)

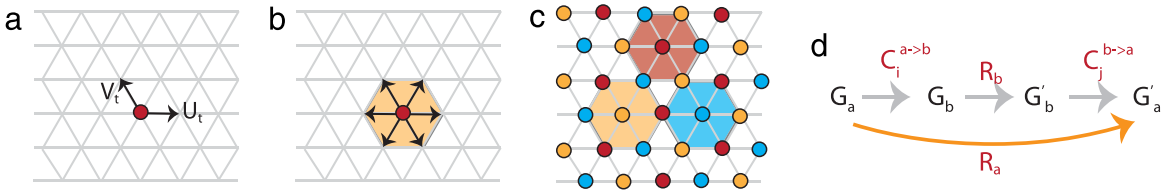

Fig. 12. (a) G_t, its origin and coordinate system. (b) Vectors chosen to aggregate a hexagonal cell in G_t. (c) Midpoints of hexagonal grids cover the entire vertices of G_t. There are three possibilities to choose the origin of the aggregation conversion illustrated by red, orange, and blue points. (d) Defining refinement R_a for G_a using refinement R_b defined for G_b. Note that this definition follows the general multiresolution framework that has been introduced earlier. (For interpretation of the references to color in this figure legend, the reader is referred to the web version of this article.)

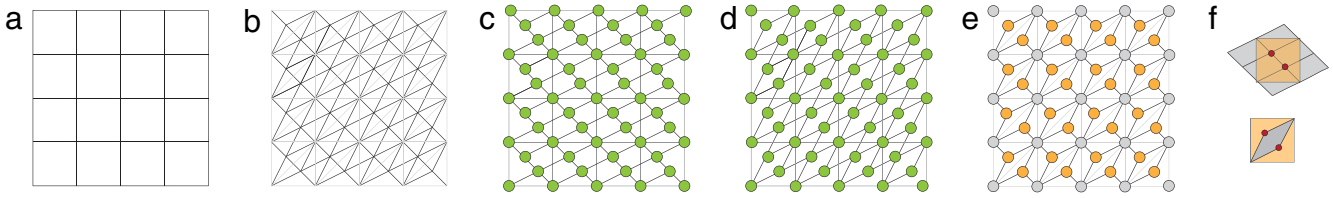

Fig. 13. (a) G_q, (b) Refined G_t by 1-to-3 refinement. (c), (d), and (e) Three types of $\acute{G}_q$ (quadrilateral 1-to-3 refinements) can be made. Note that e is a near-regular refinement. (f) Top/Bottom: Cell refinements for (c)/ (d), (e).

we can define the inverse of split conversion. Choosing other vertices as the origin has also application in finding new hexagonal refinements that we describe later in the paper.

We can apply split and aggregation conversion on any mesh. Irregular vertices in a triangular mesh would be non-hexagonal faces in the aggregated mesh with sides equal to the valence of vertices. Non-hexagonal faces also become extraordinary vertices when the split conversion is applied on a hexagonal mesh.

4.2. New refinements

Refinements are generally defined for a specific type of grid. However, using hierarchical grid conversion, we can define new refinements for grid G_a using the existing refinement for grid G_b. This happens when G_a is converted to G_b by $C_i^{a\to b}$, G_b is refined and $\acute{G}_a$ obtained by conversion $C_j^{b\to a}$. The whole process to convert G_a to $\acute{G}_a$ is a refinement R_a defined for G_a (see Fig. 12(d)). Note that transformation R_a is the combination of all transformations $C_i^{a\to b}$, R_b, and $C_j^{b\to a}$. In the following, we discuss how to obtain refinements for grids using known regular refinements for a specific type of grid.

4.2.1. Quadrilateral refinements

A variety of refinements have been proposed for quadrilateral grids. 1-to-4 refinement applied in Catmull–Clark subdivision is the most common one. However, 1-to-2 refinement used in $\sqrt{2}$ subdivision (see Appendix A) as well as 1-to-5 refinement has also been proposed for quadrilateral grids (see Appendix C) [41,42]. It is possible to extend the variety of quadrilateral refinements using defined refinements of other grids. For example, using refinements defined for triangular grids, we show how to obtain a greater variety of quadrilateral refinements.

To define quadrilateral refinements using triangular refinements, we use the sequence of conversions and refinements illustrated in Fig. 12. For instance, if we apply $C_U^{q\to t}$ and use triangular 1-to-3 refinement on G_t and then apply $C_P^{t\to q}$, the whole process is a quadrilateral 1-to-3 refinement as illustrated in Fig. 13. Note that depending on $C_P^{t\to q}$ three types of 1-to-3 refinements can be defined for quads as illustrated in Fig. 13. The result of this process may not produce a regular refinement as quadrilateral cells may have valence three or six instead of four (see Fig. 13(e)). However, there exists a strong regularity among the cells since all the cells have the same shape and area and the area of cells is compressed with the same proportion of regular refinements. Note that the area of rhombic cells is equal to $\frac{A}{3}$ where A is the area of a regular quadrilateral cell. As some properties of such refinements are the same as regular refinements, we call them *near-regular* refinements. These refinements have been also called semiregular in the literature [21]. However, to avoid confusion between semiregular models that are composed of regular patches and semiregular refinements that resemble some of the properties of regular refinement, we use the term near-regular for these refinements throughout the paper.

Quadrilateral cells can be transformed to rhombic cells using a simple matrix transformation R. Matrix $R = \begin{pmatrix} \frac{2}{3} & \frac{1}{3} \\ \frac{1}{3} & \frac{2}{3} \end{pmatrix}$ is obtained for quadrilateral 1-to-3 refinement. Note that rows of matrix R are the coordinates of new inserted points after the refinement. The refinement illustrated in Fig. 13(e) produces vertices with

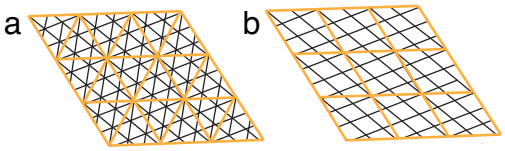

Fig. 14. 1-to-7 refinement for triangular and quadrilateral grids.

valence three or six, so we call it *3–6* refinement. It is possible to define other quadrilateral refinements based on the hierarchical grid conversion. Similarly, we can define a 1-to-7 quadrilateral refinement (see Appendix D) if we replace 1-to-3 triangular refinement by 1-to-7 triangular refinement in the conversion (Fig. 14).

4.2.2. Triangular refinements

Although triangular refinements are very well studied, we can define new refinements for triangular grids using quadrilateral refinements. Two instances of quadrilateral refinements are 1-to-2 and 1-to-5 refinements defined for quads (see Appendices A and C). To apply quadrilateral refinement R_q on a triangular grid G_t, we use pairing conversion $C_P^{t\to q}$ to obtain G_q, and then apply R_q on G_q to obtain $\acute{G}_q$. We can then apply the unpair conversion $C_U^{q\to t}$ to get $\acute{G}_t$ which is the refined version of G_t. Figs. 15 and 16 illustrate this process when R_q is 1-to-2 or 1-to-5. Note that two types of $\acute{G}_t$ can be obtained: 4–8 refinement and triangular 1-to-2 refinement.

4.2.3. Hexagonal refinement

Hexagonal refinements are often used in subdivision surfaces or image processing [8,40]. Using existing triangular refinements and our conversion technique, the number of hexagonal refinements can be expanded. Given a hexagonal grid G_h, we convert G_h to G_t using split conversion ($C_S^{h\to t}$). We then apply triangular refinement on G_t (see Fig. 17) and make a new hexagonal grid $\acute{G}_h$ using one of the aggregation conversions ($C_A^{t\to h}$). It is possible to define hexagonal refinements using a variety of triangular refinements. Fig. 18 illustrates hexagonal 1-to-4, and 1-to-7 refinements. We have three possible aggregation conversions and each produces a different refinement.

Our framework is general enough to introduce more variety of refinements by changing conversions and refinements. Here, we have provided a set of examples to describe the framework. Another instance of these refinements is produced when we use duality conversion and 1-to-2 refinement on the triangular grid, we can define a 1-to-2 refinement for hexagons as illustrated in Fig. 19. In this paper, in addition to introducing a general framework to define refinements for grids, we achieved refinements that are novel to our knowledge. Examples of these novel refinements are primal 1-to-7, and 1-to-2 hexagonal refinements, 1-to-3 and 1-to-7 quadrilateral refinements as well as 1-to-2 and 1-to-5 triangular refinements.

Although some of the refinements that are proposed seem skewed after one iteration of the refinement, it is possible to cancel out these effects after an additional application of refinements. This way, a perfect regular grid is obtained. For instance, Fig. 20 illustrates how a perfect grid is obtained after two iterations of the refinement in Fig. 13.

5. Indexing semiregular models

A semiregular model is created by applying refinements on a mesh with arbitrary connectivity. It is desired to have an efficient data structure for these meshes. In [10,11], a data structure called Atlas of Connectivity Maps (ACM) has been proposed for triangular and quadrilateral semiregular models. In this section, we discuss how to use hierarchical grid conversions to extend ACM to hexagons and also some new refinements that have not been discussed in [10,11]. Note that ACM is an example of a hierarchical data structure defined on a particular grid (quads) and it can be extended to other cells thanks to the hierarchical grid conversions proposed in this paper. We can use the same concept to extend other hierarchical data structures such as quadtrees to support other types of cells and refinements.

5.1. Review of ACM

A semiregular model consists of a number of regular patches connected to each other. In ACM, the connectivity of each patch can be captured by a simple 2D grid with a 2D indexing method and then the geometry of vertices can be recorded in a 2D array. The indexing is based on a simple coordinate system assigned to each 2D grid.

Connections within each patch are implicit and therefore connectivity queries between internal vertices of each patch are addressed by simple neighborhood vectors that connect a vertex or cell to its neighboring vertices or cells. A transformation is used to traverse from one patch to another (Fig. 21). These simple 2D patches and their interconnections are maintained through the resolutions (for all types of refinements) by applying

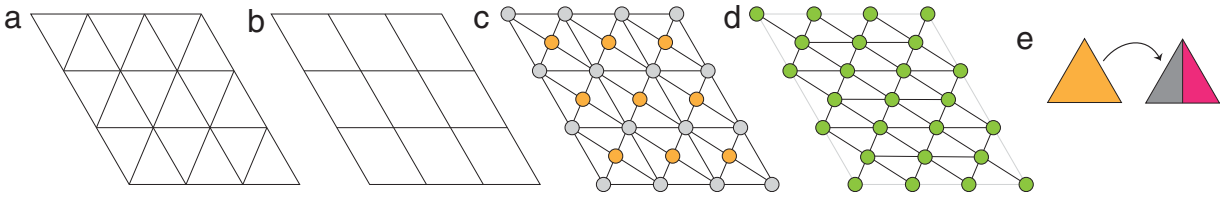

Fig. 15. (a) G_t. (b) G_q. (c) $\acute{G}_t$ (4–8 refinement). (d) $\acute{G}_t$ (triangular 1-to-2 refinement). (e) 1-to-2 cell refinement for triangles.

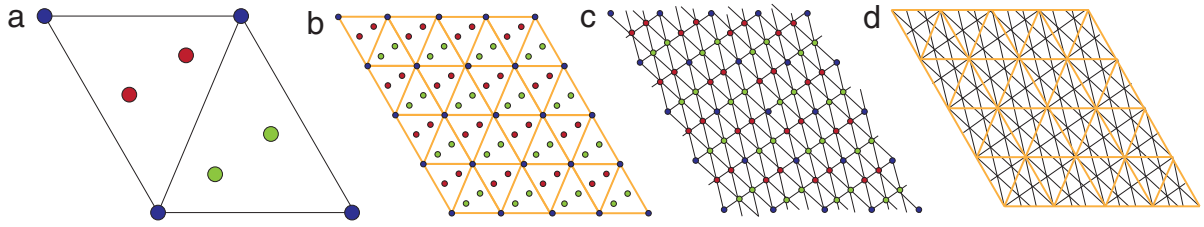

Fig. 16. (a) The location of inserted vertices. (b) New vertices on a coarse grid. (c) New edges are drawn. (d) Triangular 1-to-5 refinement.

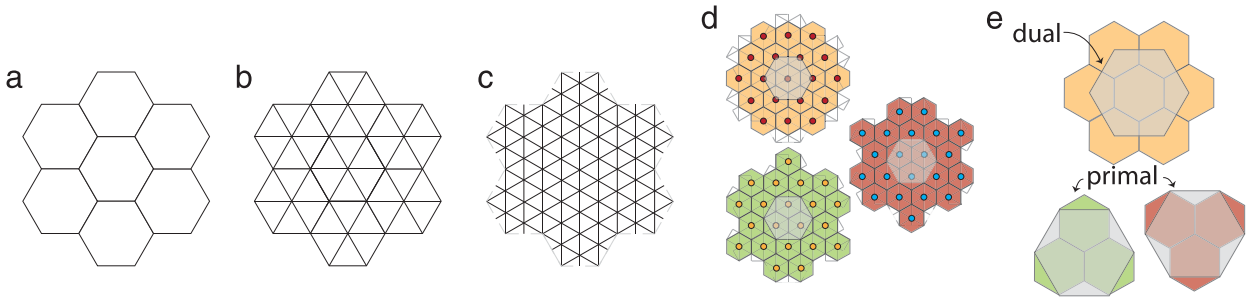

Fig. 17. (a) Hexagonal grid G_h. (b) Split conversion is applied on G_h and G_t is obtained. (c) 1-to-3 on G_t results in triangular grid $\acute{G}_t$. (d) There are three possible origins for the hexagons. (e) Choosing different origins results three distinct hexagonal refinement, one dual and two primal.

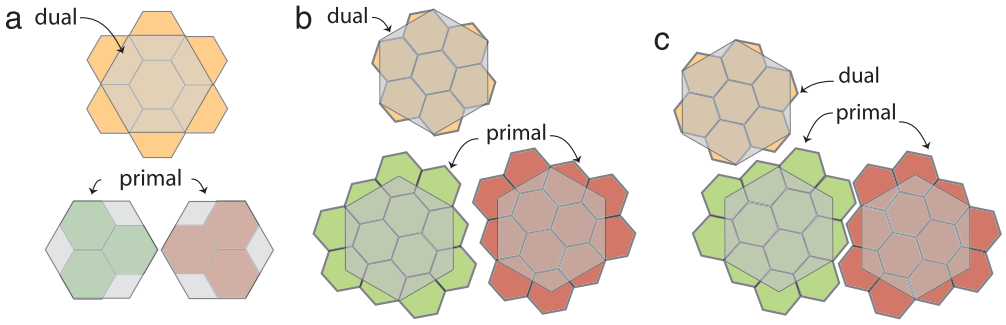

Fig. 18. Dual and primal 1-to-4 hexagonal refinements (a), 1-to-7 hexagonal refinements with 19° (b) and −19° (c) rotations.

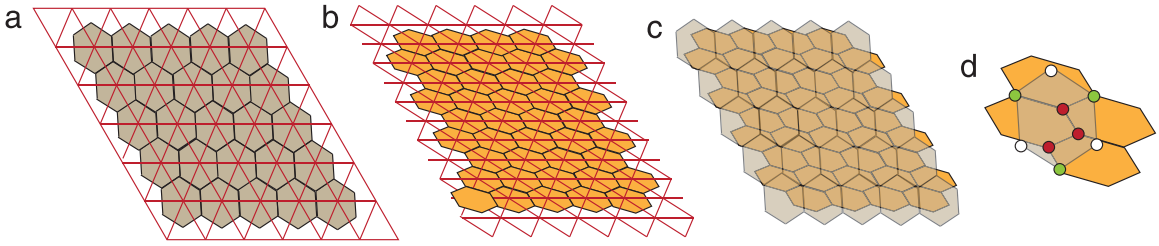

Fig. 19. (a) G_h and its dual G_t. (b) $\acute{G}_h$ and its dual $\acute{G}_t$ refined by 1-to-2 refinement. (c) G_h and $\acute{G}_h$ on top of each other. (d) Cell 1-to-2 hexagonal refinement. Red vertices are newly inserted, white vertices are removed, and green vertices are preserved after a refinement. (For interpretation of the references to color in this figure legend, the reader is referred to the web version of this article.)

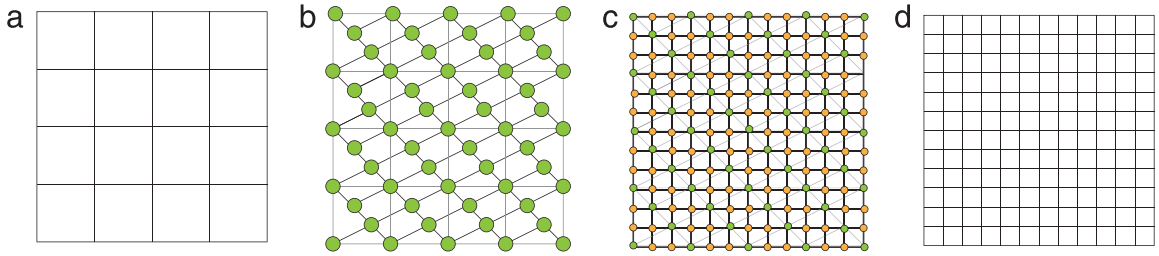

Fig. 20. (a) A quadrilateral grid. (b) 1-to-3 refinement on the quadrilateral grid in (a). (c) An additional application of 1-to-3 refinement on the grid in (b). (d) The result of two applications of 1-to-3 refinement on a quadrilateral grid is a regular quadrilateral grid.

a transformation (imposed by the refinement) to the coordinate system of each 2D patches. To capture this information, ACM has a set of elements illustrated in Fig. 21(c). Using pairing conversion $C_P^{t\to q}$, ACM can be also used for triangular refinements.

Connectivity information of a mesh is captured in a list of connectivity maps called *CM_List*. Each entry of *CM_List* (*CM_List*[*i*]) corresponds to a patch (CM_i) in the mesh. A global integer called *resolution* is also stored for the entire mesh that refers to the resolution or the level of refinement of the mesh. If we want to support adaptive subdivision with patches at different resolutions, we can separately store the resolution of each patch [43]. The resolution of the mesh helps to determine the range of vertex indices in CM_i. For example, in 1-to-4 refinement, $(a, b)_r$ are in the range $0 \le a, b \le 2^r$.

Each connectivity map CM_i has structures to store the 3D locations of its vertices and connectivity information of its neighboring patches. CM_i has a 2D location array of 3D points (x, y, z) called *vertices* storing locations of its vertices. To access neighbors, each CM_i has also an integer array called *neighbors* that keeps the indices of the neighbors of CM_i in *CM_List*. For each neighbor ($CM_{i\alpha}$), a $T_{i\alpha}$ is also stored in an array called *transformation*. To have an easier representation for transformations, we encode possible $T_{i\alpha}$ by integers. These transformations are used to traverse from one patch to its neighboring patches.

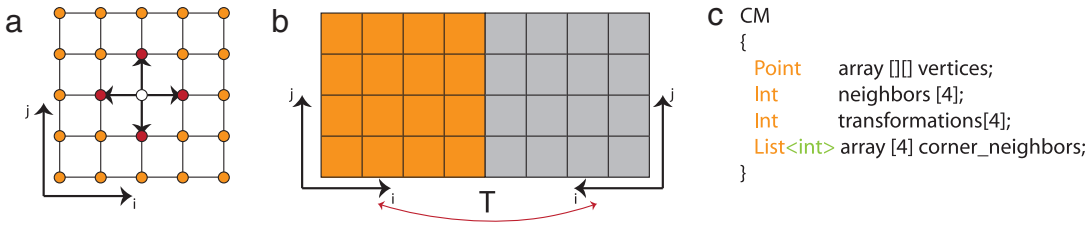

Fig. 21. (a) A connectivity map. Vertices are connected to their neighbors by neighborhood vectors. (b) Transformation T is used to traverse from one connectivity map to its neighbors. (c) Elements of a connectivity map. In ACM, we have a list of connectivity maps (CM) for the entire model.

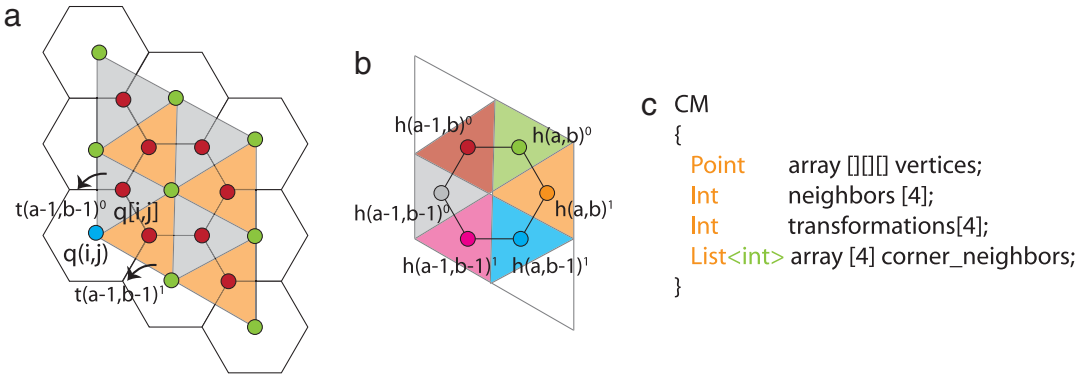

Fig. 22. (a) Vertices of a quadrilateral and hexagonal patch are drawn in green and red respectively. Vertex $q(i, j)$ (drawn in blue) is the bottom-left corner of cell $q[i, j]$. Cell $q[i, j]$ is split into two triangles $t[i, j]^0$, and $t[i, j]^1$ illustrated in gray and orange respectively (b) Vertices of a hexagon and their associated triangular cells. (c) Modified ACM for vertices of hexagonal cells. We use a 3D array instead of 2D arrays for storing vertices. (For interpretation of the references to color in this figure legend, the reader is referred to the web version of this article.)

Irregular vertices in semiregular meshes are only found at the corners of the connectivity maps. These vertices are shared by multiple connectivity maps. Therefore, to access the neighbors of a corner, we store patches that share the same corner.

The reason for having an advantage over other common data structures for storing the connectivity of a mesh such as half-edges is that in ACM the connectivity information of vertices, faces, and edges are not stored throughout the resolutions [10,11]. The only stored information of the mesh is the connectivity of the first resolution which is constant throughout the resolutions. In addition, handling the neighborhood finding operation using simple algebraic operations such as neighborhood vectors enhances the performance of ACM in applications with extensive dependency to the connectivity information of vertices such as subdivision.

5.2. ACM for hexagons

As ACM is an efficient data structure for semiregular models, it is desired to use it for hexagonal cells, despite its original formulation in terms of triangles and quads. Hierarchical grid conversions provided in this paper can help to extend ACM for supporting hexagons. To apply ACM to hexagons, we use dual conversion $C_D^{h\to t}$ and obtain a triangular patch with $n\times n$ vertices from an $n\times n$ patch of hexagonal cells (Fig. 22(a)). This way, for each triangular cell, a unique vertex of hexagonal cells exists (Fig. 22(b)). A quadrilateral patch with $n\times n$ vertices can be represented by a 2D array in which the (i, j) entry of the array refers to the bottom-left vertex of cell $q[i, j]$ (see Fig. 22(a)). As discussed earlier, each quad $q[i, j]$ may be split into triangular cells $t[i, j]^0$ and $t[i, j]^1$. Each triangular cell $t[i, j]^k$ ($k = 0$ or 1) corresponds to a vertex in a hexagonal grid. As a result, vertices of a hexagonal grid are represented in a 3D array in which entry (i, j, k) refers to triangular cell $t[i, j]^k$ obtained from dual conversion of the hexagonal grid.

We can modify the location array of vertices in ACM to a 3D array to support hexagonal grids (see Fig. 22(c)). Transformation between connectivity maps and handling the neighborhood queries are similar to the case of triangular cells. Fig. 23 illustrates a hexagonal mesh at two successive resolutions and its connectivity maps. By extending ACM to support hexagonal grids, we can benefit from the advantages of ACM, such as speed in handling connectivity queries and the efficient support of hierarchical queries between the vertices and cells.

5.3. ACM refinement extension

In [10,11], only regular refinements (with specific rotation) have been discussed. By providing more possible refinements through hierarchical grid conversions, the question is how to extend ACM to support these refinements. Here, we discuss how ACM can be modified to support more variety of refinements. In the following, we discuss two categories of refinements that have not been explored in [10,11].

1-to-5 and 1-to-7: In [10], refinements are categorized based on their imposed transformation to the grid of subsequent resolutions. Based on these categorizations, both 1-to-5 and 1-to-7 refinements belong to the category – scaling, rotation, no translation – that means these refinements impose only scaling and rotation to the subsequent grids. In ACM, rotation of refinements is eliminated in order to benefit from the connectivity information of the first resolution. In [10], 1-to-2 refinement is presented as an instance of this category by scaling the connectivity map by two. This way, at odd resolutions, some empty indices exist that are filled by new vertices at the next even resolution. In fact, after two resolutions, the connectivity maps are simply scaled by two without any rotation involved. This works due to the cancellation of the 45° rotation of 1-to-2 refinement after two resolutions.

1-to-5 and 1-to-7 refinements are not aligned after two resolutions since the rotations are not canceled out. However, two versions of these refinements exist with θ and $-\theta$ rotations (see Fig. 24). To have aligned connectivity maps for these refinements,

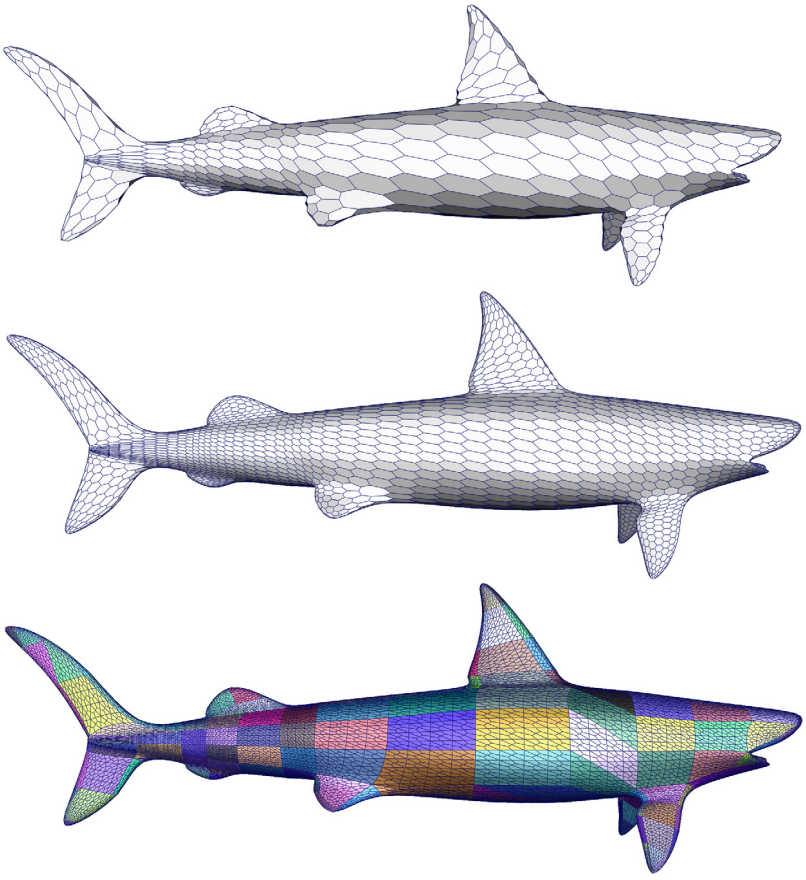

Fig. 23. A shark at two successive resolutions (top) and its corresponding connectivity maps at the bottom.

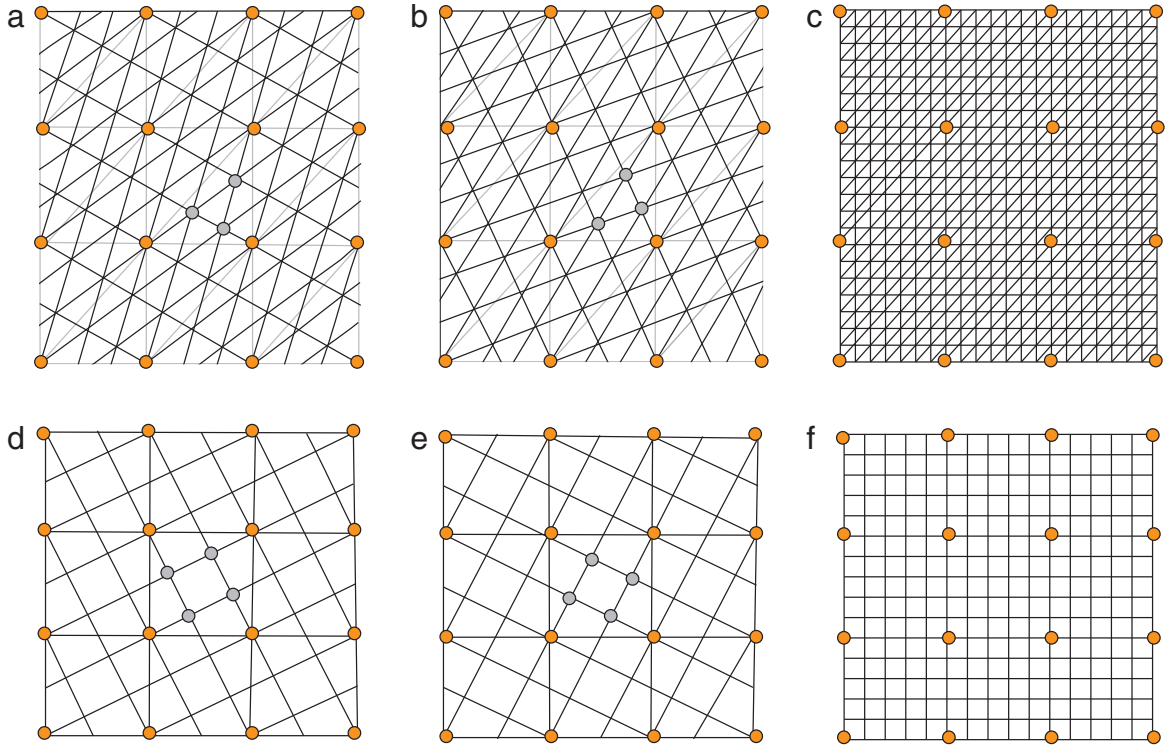

Fig. 24. (a), (b) 1-to-7 refinement with $+19^\circ$ and -19° rotations. (c) After one level of refinement in (a) followed by the refinement in (b), the rotation is discarded. (d), (e) 1-to-7 refinement with $+25^\circ$ and -25° rotations. (f) Rotation is canceled out.

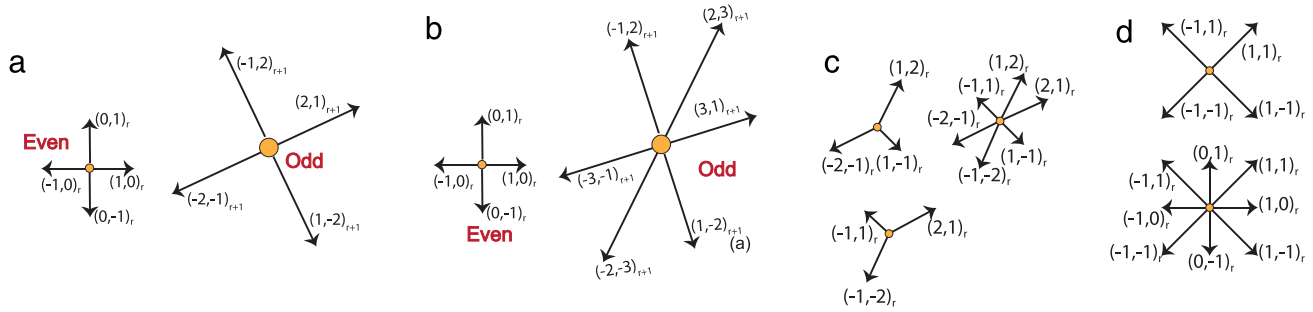

Fig. 25. Neighborhood vectors for (a) 1-to-5, (b) 1-to-7, (c) 3–6 and (d) 4–8 refinements.

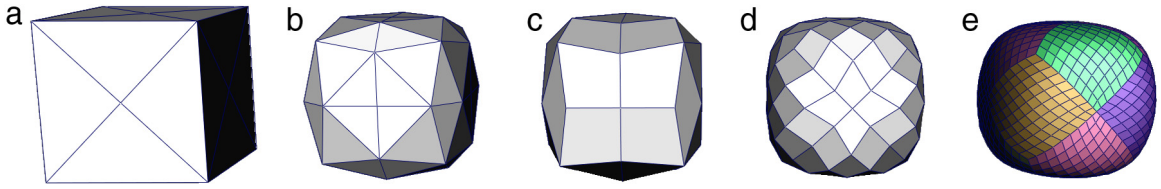

Fig. 26. (a) A triangulated cube. (b) Applying $\sqrt{3}$ subdivision on (a). (c) Applying unpair conversion on (b) results a quadrilateral mesh refined by 1-to-3 and smoothed by $\sqrt{3}$ subdivision. (d) Applying the same process (unpair conversion and smoothing) on (c). (e) The cube in (a) after applying 1-to-3 refinement and $\sqrt{3}$ smoothing masks.

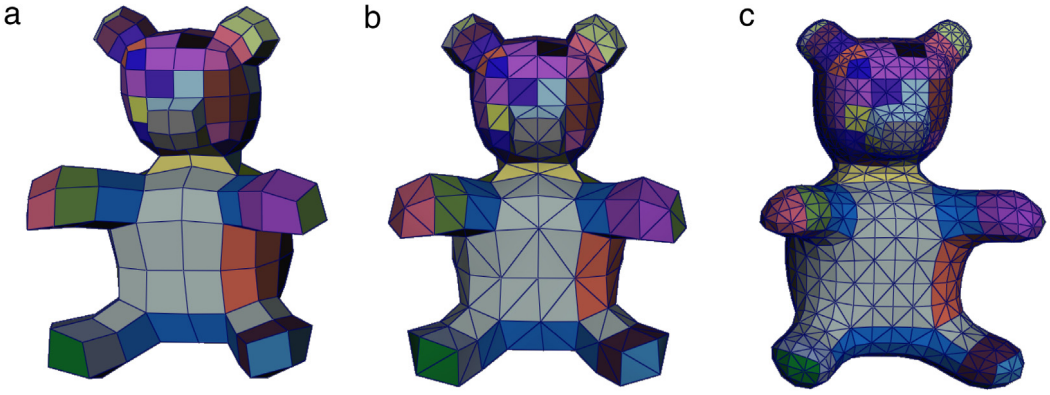

Fig. 27. (a) A quadrilateral mesh. (b) Triangulating the mesh using pairing conversion. (c) 4–8 subdivision using ACM on the triangulated mesh.

we can apply one level of refinement with θ followed by one level of refinement with $(-\theta)$ rotation. This way, rotations are canceled out, and we get a refinement with the same factor but without a rotation (see Fig. 24). Note that neighborhood vectors that connect a vertex to its neighbors are different for even and odd resolutions in refinements that impose rotations. Fig. 25(a) and (b) show neighborhood vectors for 1-to-5 and 1-to-7 refinements.

4–8 and 3–6: 4–8 and 3–6 near-regular refinements have two types of neighborhood vectors based on the type of vertex. Fig. 25(c) and (d) illustrate neighborhood vectors for vertices of 4–8 or 3–6 refinement. Connectivity maps are scaled by two and three every other resolution for 4–8 and 3–6 refinements respectively (see Fig. 27).

6. Discussion and results

Using the hierarchical grid conversions, we can define new refinements that may be applied on regular grids. By alternating between conversions and refinements, we can also apply subdivision methods that are defined for specific results. For example, we can apply 1-to-3 refinement on quadrilateral grids with the smooth filters defined for the $\sqrt{3}$ subdivision method for triangular grids (see Fig. 26). We also extend ACM to support hexagonal meshes (see Fig. 23) as well as more variety of refinements such as, 1-to-7, 1-to-5, and 4–8 subdivision (Fig. 27). As a result, ACM, which efficiently handles connectivity and hierarchical queries on semiregular models, can be applied to a greater variety of refinements and grid types. Note that the smoothness of these subdivision techniques is the same as the original underlying subdivision (e.g. $\sqrt{3}$ for Fig. 26 and 4–8 subdivision for Fig. 27) as the conversions do not change the geometry and they just change the connectivity of vertices. Extraordinary vertices of the mesh are also limited to the number of extraordinary vertices at the first resolution after conversions and they have the same as smoothness of extraordinary vertices in the underlying subdivision. Our proposed conversions can also be used to efficiently switch between grids as needed by the application. For example, the hexagonal meshes that are common in Earth representations [44–46] can be converted to a triangular mesh for efficient rendering (see Fig. 28).

Although the focus of the paper is to study conversions for regular grids or semiregular meshes that are composed of attached bounded grids, it is interesting to see what are the outputs of each conversion in case of different input meshes. In general, if the input of a conversion is not a regular mesh, the result of the conversion is not usually a regular mesh. Note that defining a coordinate system for an irregular mesh and therefore establishing transformations are not as straightforward as regular grids. However, if the mesh is pure quad or triangle mesh, we can still apply refinements and use ACM to support its connectivity and hierarchical queries. Table 1 shows the output of each conversion having different

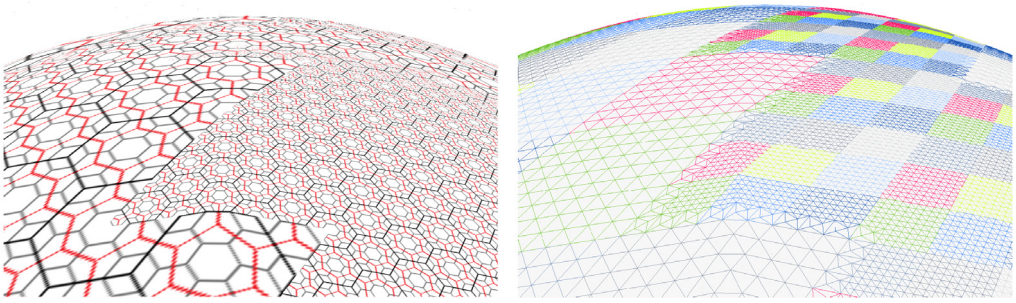

Fig. 28. Left: A hexagonal globe with 1-to-3 refinement at three successive resolutions. Right: Triangulation of left using dual conversion using ACM.

Table 1
Inputs and output of the discussed conversions. Note that irregular mesh is a mesh whose face can have arbitrary number of sides. *im* in the superscript of conversions refers to irregular meshes. Irregular quad and irregular triangle also respectively indicate meshes with only quads or triangles whose vertices can be of arbitrary valence.

Conversion	Input	Output
$C_P^{t->q}$	Regular triangle	Regular quad
$C_P^{t->q}$	Irregular triangle (spherical topology)	Irregular quad
$C_P^{t->q}$	Irregular triangle (non-spherical topology)	Quad and triangle
$C_U^{q->t}$	Regular quad	Regular triangle
$C_U^{q->t}$	Irregular quad	Irregular triangle
$C_U^{q->t}$	Quad and triangle	Irregular triangle
$C_D^{t->h}$	Regular triangle	Regular hexagon
$C_D^{h->t}$	Regular hexagon	Regular triangle
$C_D^{q->q}$	Regular quad	Regular quad
$C_D^{im->im}$	Irregular mesh	Irregular mesh
$C_S^{h->t}$	Regular hexagon	Regular triangle
$C_S^{h->t}$	Irregular hexagon	Irregular triangle
$C_A^{t->h}$	Regular triangle	Regular hexagon
$C_A^{t->im}$	Irregular triangle	Irregular mesh

inputs. For example, when a triangular mesh has a boundary, it may not be impossible to obtain a pure quad mesh with no isolated triangle at the boundaries as the mesh may have odd number of triangles or the connectivity of triangles does not allow a pure quadrangulation. By following this table, we can also find the output of a combination of conversions. For example, if we have an input irregular hexagonal mesh M_h and apply split conversion, $C_S^{h\to t}$, to it, we obtain an irregular triangular mesh M_t. Now, we can apply pairing conversion, $C_P^{t\to q}$, to M_t. Based on whether M_t (equivalently M_h) has a spherical topology, we can obtain pure irregular quadrilateral mesh or a mix of triangles and quads.

7. Conclusion and future work

In this paper, we present hierarchical grid conversions and use it to systematically define refinements. We extend an existing patch-based hierarchical data structure called ACM for handling connectivity queries of semiregular models, to support hexagonal semiregular models and some additional refinements. From this enhanced support and newly defined conversions, we can best apply a given grid-type to the application-specific challenge.

Based on the conversions between regular grids, we can extend ACM to support hexagonal semiregular models as well as a wider range of refinements such as 4–8 and 1-to-7 refinements. We have proposed new types of refinements that may be used to generate smooth subdivision schemes. Finding smoothing masks of these new refinements and their multiresolution filters can be a future work. ACM is designed for semiregular models and models obtained from adaptively subdividing patches. Extending ACM to support meshes that have a combination of regular patches and irregular connectivity is also a future work. One possibility is to combine ACM with a known data structure such as half-edges that can perform well for irregular patches of the mesh.

Acknowledgments

We would like to thank anonymous reviewers for their insightful comments. This research was supported in part by PYXIS Innovation Inc. (grant number: 10010807) and National Science and Engineering Research Council of Canada providing the Collaborative Research and development funding (grant number: 10010985) and Discovery Grant (grant number: 249893-2012).

Appendix A. 1-to-2 refinement

1-to-2 refinement used in quadrilateral $\sqrt{2}$ subdivision is composed of two stages of splitting and edge-flip. In the splitting stage, a cell is split by inserting the midpoint of quadrilateral cells. These vertices are then connected to the old vertices and old edges are flipped (see Fig. A.29).

Appendix B. 1-to-3 refinement

1-to-3 refinement is used in $\sqrt{3}$ subdivision [47]. In this refinement, a vertex is inserted in the midpoint of each cell. These newly inserted vertices are connected to the old vertices by inserting new edges and old edges are flipped (see Fig. B.30). Fig. B.30 illustrates the steps of 1-to-3 refinement.

Appendix C. 1-to-5 refinement

1-to-5 refinement has been introduced for quadrilateral grids. In this refinement, four vertices at locations $\left(\frac{2}{5}, \frac{1}{5}\right)$, $\left(\frac{4}{5}, \frac{2}{5}\right)$, $\left(\frac{1}{5}, \frac{3}{5}\right)$, and $\left(\frac{3}{5}, \frac{4}{5}\right)$ are inserted. The connectivity of vertices is changed afterwards as illustrated in Fig. C.31.

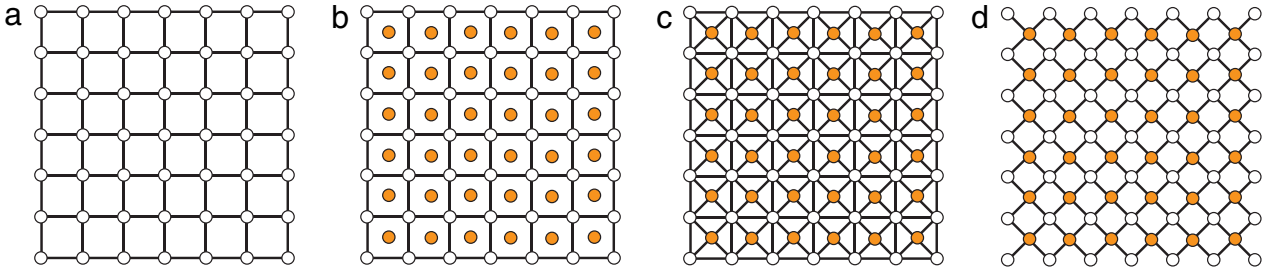

Fig. A.29. (a) A quadrilateral grid. (b) Midpoints of cells are inserted. (c) New edges are drawn. (d) Old edges are removed.

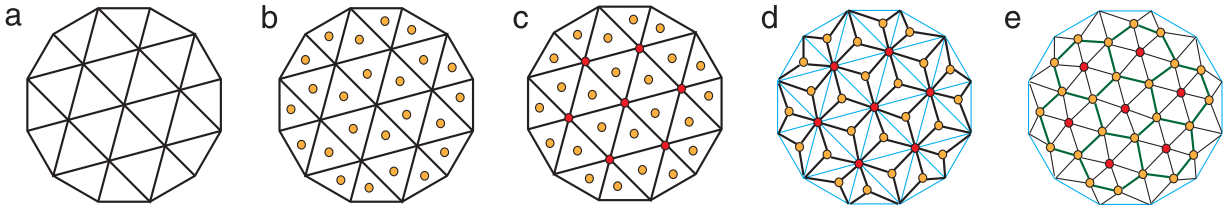

Fig. B.30. (a) A triangular grid. (b) Midpoints of each triangular cell are inserted. (c) Old vertices are drawn in red. (d) New vertices are connected to old vertices. (e) Old edges are flipped. (For interpretation of the references to color in this figure legend, the reader is referred to the web version of this article.)

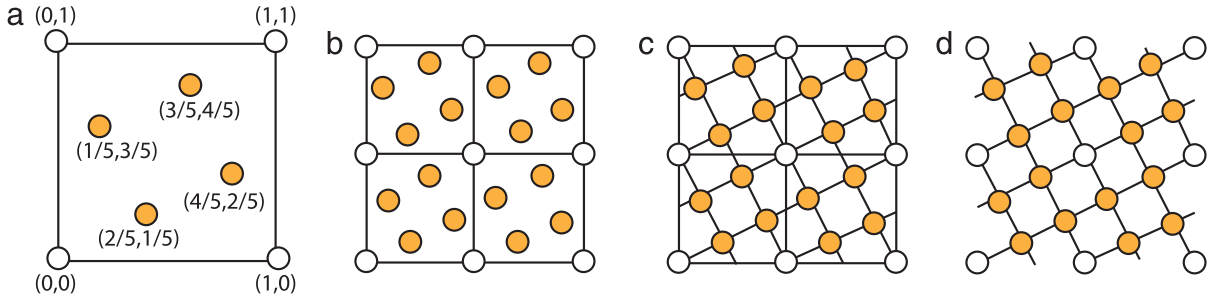

Fig. C.31. (a) The location of inserted vertices. (b) New vertices on a coarse grid. (c) New edges are drawn. (d) Old edges are removed.

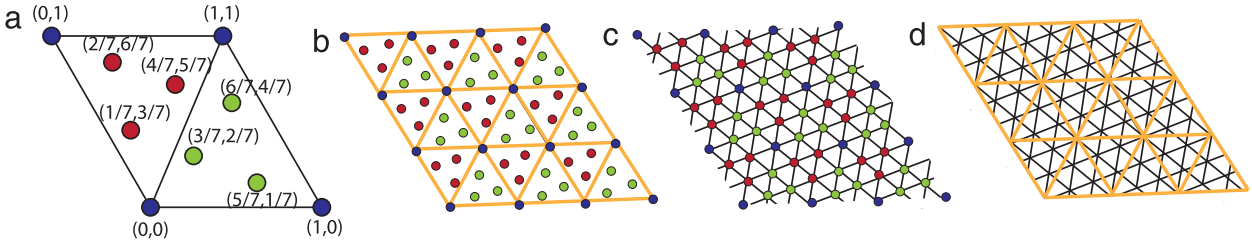

Fig. D.32. (a) Masks of 1-to-7 refinement. (b) New vertices are inserted. (c) Old edges are removed and new and old vertices are connected. (d) Orange coarse triangular grid is refined by 1-to-7 refinement.

Appendix D. 1-to-7 refinement

1-to-7 triangular refinement has been studied in $\sqrt{7}$ subdivision [42]. In this refinement, three vertices are inserted in a triangular cell, old edges are removed and new edges are formed. Consider a diamond with unit length edges. In triangle $t[0, 0]^0$, three vertices with coordinates $\left(\frac{1}{7}, \frac{3}{7}\right)$, $\left(\frac{4}{7}, \frac{5}{7}\right)$, and $\left(\frac{2}{7}, \frac{6}{7}\right)$ are inserted and in $t[0, 0]^1$, coordinates of three new vertices are $\left(\frac{5}{7}, \frac{1}{7}\right)$, $\left(\frac{3}{7}, \frac{2}{7}\right)$, and $\left(\frac{6}{7}, \frac{4}{7}\right)$. Fig. D.32 illustrates the mask of 1-to-7 refinement and its topological changes.

References

[1] de Berg M, van Kreveld M, Overmars M, Schwarzkopf O. Computational geometry: Algorithms and applications. 2nd ed. Springer-Verlag; 2000.
[2] Loop C. Smooth subdivision surfaces based on triangles, The University of Utah, Department of Mathematics, 1987.
[3] Piegl L, Tiller W. The NURBS book. 2nd ed. New York, (NY), (USA): Springer-Verlag New York, Inc.; 1997.
[4] Catmull E, Clark J. Recursively generated B-spline surfaces on arbitrary topological meshes. Comput-Aided Des 1978;10(6):350–5.
[5] Samet H. Foundations of multidimensional and metric data structures. The Morgan Kaufmann series in computer graphics and geometric modeling, San Francisco, CA, USA: Morgan Kaufmann Publishers Inc.; 2005.
[6] He X. et al. Hexagonal structure for intelligent vision. In: First international conference of information and communication technologies, ICIT 2005, 2005, pp. 52–64.
[7] Sahr K. Location coding on icosahedral aperture 3 hexagon discrete global grids, Computers. Environ Urban Syst 2008;32(3):174–87.
[8] Claes J, Beets K, Van Reeth F. A corner-cutting scheme for hexagonal subdivision surfaces. In: Proceedings of the shape modeling international 2002 (SMI'02). SMI'02, Washington, DC, USA: IEEE Computer Society; 2002. p. 13–20.
[9] Weiss K, De Floriani L. Simplex and diamond hierarchies: Models and applications. Comput Graph Forum 2011;30(8):2127–55.

[10] Mahdavi-Amiri A, Samavati F. ACM: Atlas of connectivity maps for semiregular models. In: Proceedings of graphics interface 2013, 2013, pp. 99–107.
[11] Mahdavi-Amiri A, Samavati F. Atlas of connectivity maps. Comput Graph 2014; 39:1–11.
[12] Lindstrom P, Koller D, Ribarsky W, Hodges LF, Faust N, Turner GA. Real-time, continuous level of detail rendering of height fields. In: Proceedings of the 23rd annual conference on Computer graphics and interactive techniques, SIGGRAPH'96, 1996, pp. 109–118.
[13] Guenette M, Stewart AJ. Triangulation of hierarchical hexagon meshes. In: Proceedings of the 2008 ACM symposium on Solid and physical modeling, SPM'08, 2008, pp. 307–313.
[14] Bommes D, Levy B, Pietroni N, Puppo E, Tarini CSa,M, Zorin D. State of the art in quad meshing. In: Eurographics STARS. 2012.
[15] Akleman E, Srinivasan V, Mandal E. Remeshing schemes for semi-regular tilings. In: Proceedings of the international conference on shape modeling and applications 2005, SMI'05, 2005, pp. 44–50.
[16] Bo P, Pottmann H, Kilian M, Wang W, Wallner J. Circular arc structures. ACM Trans Graph 2011;30(4):101:1–101:12.
[17] Schiftner A, Höbinger M, Wallner J, Pottmann H. Packing circles and spheres on surfaces. In: ACM SIGGRAPH Asia 2009 papers, SIGGRAPH Asia'09, 2009, pp. 139:1–139:8.
[18] Nieser M, Palacios J, Polthier K, Zhang E. Hexagonal global parameterization of arbitrary surfaces. In: ACM SIGGRAPH ASIA 2010 sketches, SA'10, 2010, pp. 5:1–5:2.
[19] Oswald P, Schröder P. Composite primal/dual $\sqrt{3}$ subdivision schemes. Comput Aided Geom Design 2003;20(3):135–64.
[20] Guskov I, Khodakovsky A, Schröder P, Sweldens W. Hybrid meshes: Multiresolution using regular and irregular refinement. In: Proceedings of the eighteenth annual symposium on computational geometry. SCG'02, New York, (NY), (USA): ACM; 2002. p. 264–72.
[21] Velho L. Semi-regular 4–8 refinement and box spline surfaces. In: Proceedings XIII Brazilian symposium on Computer graphics and image processing, 2000., 2000, pp. 131–138.
[22] Peters J, Reif U. The simplest subdivision scheme for smoothing polyhedra. ACM Trans Graph 1997;16(4):420–31.
[23] Alexa M. Refinement operators for triangle meshes. Comput Aided Geom Design 2002;19(3):169–72.
[24] Ivrissimtzis IP, Dodgson NA, Sabin MA. A generative classification of mesh refinement rules with lattice transformations. Comput Aided Geom Design 2004;21(1):99–109.
[25] Dodgson N. An heuristic analysis of the classification of bivariate subdivision schemes. In: Martin R, Bez H, Sabin M, editors. Mathematics of surfaces XI. Lecture notes in computer science, vol. 3604. Berlin, (Heidelberg): Springer; 2005. p. 161–83.
[26] Destelle F, Gérot C, Montanvert A. A topological lattice refinement descriptor for subdivision schemes. In: Proceedings of the 7th international conference on mathematical methods for curves and surfaces. MMCS'08, Springer-Verlag; 2010. p. 153–77.
[27] Vince A, Zheng X. Arithmetic and Fourier transform for the PYXIS multi-resolution digital earth model. Int J Digital Earth 2009;2(1):59–79.
[28] Mahdavi-Amiri A, Bhojani F, Samavati F. One-to-two digital earth. In: 9th International symposium on visual computing (ISVC 2013). Lecture notes in computer science, vol. 8034. Springer; 2013.
[29] Zorin D, Schröder P, Sweldens W. Interactive multiresolution mesh editing. In: Proceedings of the 24th annual conference on computer graphics and interactive techniques. SIGGRAPH'97, ACM Press, Addison-Wesley Publishing Co.; 1997. p. 259–68.
[30] Olsen L, Samavati F, Bartels R. Multiresolution for curves and surfaces based on constraining wavelets. Comput Graph 2007;31(3):449–62.
[31] Weiler K. Edge-based data structures for solid modeling in curved-surface environments. IEEE Comput Graph Appl 1985;5(1):21–40.
[32] Kraemer P, Cazier D, Bechmann D. Extension of half-edges for the representation of multiresolution subdivision surfaces. Vis Comput 2009;25:149–63.
[33] Gargantini I. An effective way to represent quadtrees. Commun ACM 1982; 25(12):905–10.
[34] Mahdavi-Amiri A, Samavati FF, Peterson P. Categorization and conversions for indexing methods of discrete global grid systems. ISPRS Int J Geo-Inf 2015;4: 320–36.
[35] Bertram M. Biorthogonal loop-subdivision wavelets. Computing 2004; 72(1–2):29–39.
[36] Mahdavi-Amiri A, Samavati F. Connectivity maps for subdivision surfaces. In: GRAPP/IVAPP. 2012. p. 26–37.
[37] Petersen J. Die theorie der regulären graphs. Acta Math 1891;15:193–220.
[38] Biedl TC, Bose P, Demaine ED, Lubiw A. Efficient algorithms for Petersen's matching theorem. J Algorithms 2001;38(1):110–34.
[39] Snyder WE, Qi H, Sander W. A coordinate system for hexagonal pixels. In: The international society for optical engineering, Vol. 3661, 1999, pp. 716–727.
[40] Middleton L, Sivaswamy J. Hexagonal image processing: A practical approach. Advances in Pattern Recognition, Secaucus, (NJ), (USA): Springer-Verlag, New York, Inc.; 2005.
[41] Ivrissimtzis I, Dodgson N, Sabin M. $\sqrt{5}$ subdivision. In: Dodgson N, Floater M, Sabin M, editors. Advances in multiresolution for geometric modelling, mathematics and visualization. Berlin, (Heidelberg): Springer; 2005. p. 285–99.
[42] Chui CK, Jiang Q, Ndao RN. Triangular $\sqrt{7}$ and quadrilateral $\sqrt{5}$ subdivision schemes: Regular case. J Math Anal Appl 2008;338(2):1204–23.
[43] Mahdavi-Amiri A, Samavati F. Adaptive atlas of connectivity maps. In: Curves and surfaces—8th international conference, Paris, France, June 12–18, 2014, Revised Selected Papers, 2014, pp. 304–320.
[44] PYXIS Innovation, March 2013. URL: http://www.pyxisinnovation.com.
[45] Mahdavi-Amiri A, Harrison E, Samavati F. Hexagonal connectivity maps for digital Earth. Int J Digit Earth 2014;1–20.
[46] Mahdavi-Amiri A, Alderson T, Samavati F. A survey of digital earth. Comput Graph 2015;53(Part B):95–117. http://dx.doi.org/10.1016/j.cag.2015.08.005. URL: http://www.sciencedirect.com/science/article/pii/S0097849315001399.
[47] Kobbelt L. $\sqrt{3}$ subdivision. In: SIGGRAPH'00: Proceedings of the 27th annual conference on Computer graphics and interactive techniques, 2000, pp. 103–112.